Strength softening mitigation in bimodal structured metals •

Cite as: J. Appl. Phys. 131, 045102 (2022); https://doi.org/10.1063/5.0075475 Submitted: 15 October 2021 • Accepted: 28 December 2021 • Published Online: 24 January 2022

🗓 Han Wang and 🗓 Penghui Cao

COLLECTIONS

This paper was selected as Featured







ARTICLES YOU MAY BE INTERESTED IN

Uniqueness of parameter estimates obtained from fitting free carrier absorption data of silicon wafers

AIP Advances 11, 105003 (2021); https://doi.org/10.1063/5.0059258

Intrinsically shunted Josephson junctions with high characteristic voltage based on epitaxial NbN/TaN/NbN trilayer

Applied Physics Letters 119, 152602 (2021); https://doi.org/10.1063/5.0064733

Metadamping enhancement and tunability via scissor-like electromechanical metamaterials Journal of Applied Physics 130, 184901 (2021); https://doi.org/10.1063/5.0058086





Strength softening mitigation in bimodal structured metals 6

Cite as: J. Appl. Phys. 131, 045102 (2022); doi: 10.1063/5.0075475 Submitted: 15 October 2021 · Accepted: 28 December 2021 · Published Online: 24 January 2022









Han Wang¹ and Penghui Cao^{1,2,a)}



AFFILIATIONS

- Department of Mechanical and Aerospace Engineering, University of California, Irvine, California 92697, USA
- ²Department of Materials Science and Engineering, University of California, Irvine, California 92697, USA

ABSTRACT

Polycrystalline metals become stronger with a decrease in the constitute grain size, yet strength softening takes over at the nanometer regime. Here, we find that this softening rate can be tailored and mitigated by tuning structural heterogeneity and grain size uniformity. With reducing the small grain size in bimodal structures, the strength reduction is markedly alleviated due to the enhanced strengthening of large grains. This mitigation of strength softening is mediated by promoted intragranular slip, extra dislocation storage, and reduced grain boundary sliding in bimodal structures. Our findings signifying the role of grain size non-uniformity on crystal plasticity shed light on a broad class of heterogeneous structured materials with improved strength and ductility.

Published under an exclusive license by AIP Publishing. https://doi.org/10.1063/5.0075475

I. INTRODUCTION

Most structural and functional materials are polycrystals made of a large number of single crystalline grains aggregated together. The strength of polycrystalline metals becomes stronger with reducing the size of constituent grains, known as the Hall-Petch effect. 1-3 This strengthening effect breaks down when the grain size falls into the nanometer regime and reaches a critical point, at which the strength softening takes over the strengthening and becomes the predominant mechanism. In this inverse Hall-Petch regime, 4-6 the material strength drastically decreases with a decrease in the grain size, caused by grain boundary-mediated activities such as intergranular sliding.

Recently, an arising class of heterogeneous structured materials, including bimodal, multimodal, and gradient structures, exhibited unprecedented mechanical behaviors, such as ultrahigh strength and better tensile ductility, when compared with their homogeneous counterparts. This suggests that manipulating the structural parameters provides an approach to tailoring mechanical behaviors toward desired properties. One of such successful examples is from a thermo-mechanically treated copper, consisting of a microstructure with bimodal grain size distribution (coarse grains embedded inside a matrix of nanocrystalline grains). 10 This inhomogeneous microstructure induces strain hardening mechanisms, leading to a high tensile ductility of 65% elongation to failure.

Interestingly, the bimodal structure enhanced mechanical behaviors have been found applicable to other metals, such as nickel,¹ aluminum, 13 and titanium, 14 which possess superior mechanical properties than that of homogeneous metals. It is reasonable to hypothesize that the structural heterogeneities intentionally engineered into the bimodal structured materials considerably impact deformation mechanisms. One interesting question arises as to the role of bimodal structuring in strength softening, with the influence of a bimodal structure on mechanical properties being suggested experimentally. 10,15,1

Here, we perform parallel atomistic deformation simulations of bimodal nanograined (BNG) copper with various grain size ratios. By comparing with homogeneous nanograined (HNG) copper, we find that the strength softening rate in the inverse Hall-Petch regime is markedly alleviated in bimodal structures. The mitigation of strength softening is mediated by enhanced intragranular slip, extra dislocation storage, and reduced grain boundary sliding in the bimodal structure.

II. SIMULATION MODELS

We create a series of bimodal nanograined structures with dimensions of $40 \times 40 \times 40 \text{ nm}^3$ (containing 5.5×10^6 atoms), in which the large grains and small grains equally occupy half of the system volume. In these bimodal structures, the small grain size

^{a)}Author to whom correspondence should be addressed: caoph@uci.edu

varies from 20 to 2 nm while fixing the large grain size to be 20 nm, which enables studying the effects of structural heterogeneity (i.e., grain size ratio) on mechanical strength. Figures 1(a) and 1(b) show two slices of BNG structures with large to small grain size ratios of 20:3 and 20:9, respectively. We use the embedded-atom method (EAM) potential¹⁷ to describe the interatomic interaction

of Cu atoms, and all the simulations were conducted at constant temperature 300 K using the Nosé–Hoover thermostat. ^{18,19} With periodic boundary conditions applied to all three directions, we first relax the structures at 300 K for 50 ps, followed by uniaxial tensile deformation. During mechanical deformation, we set the atoms in small and large grains to two different groups. By

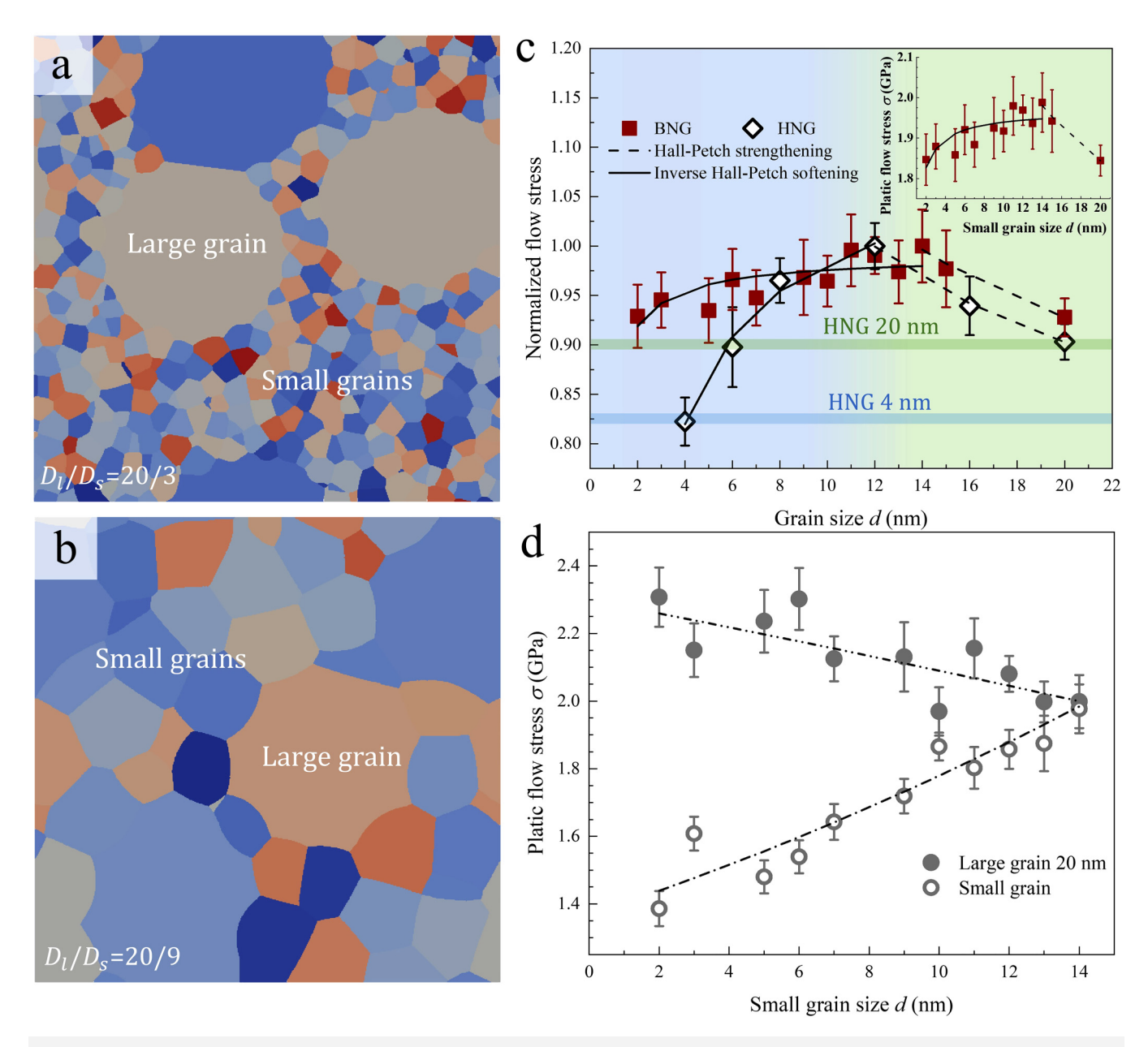


FIG. 1. Bimodal nanograined structures with grain size ratios of (a) 20:3 and (b) 20:9. The grain color is randomly assigned to show the structural morphology. (c) The averaged plastic flow stress of BNG structures compared with that of HNG structures. The flow stress is normalized by the maximum strength for comparing the softening rates between BNG and HNG. The inset shows the average plastic flow stress (raw data, unnormalized) for each BNG structure. (d) The plastic flow stresses of large and small grains in BNG structures show the stress of large grain increases with a decrease in the small grain size.

considering the atomic stresses in the two groups, the mechanical stresses associated with large and small grains can be evaluated and differentiated. The samples are stretched at a constant engineering strain rate of $5 \times 10^8 \, \text{s}^{-1}$, and the stresses in the other two directions perpendicular to tensile are controlled at zero using isothermal–isobaric (NPT) ensemble. A series of HNG structures consisting of various grain sizes are studied for comparison, and different strain rates ranging from 5×10^7 to $1 \times 10^{10} \, \text{s}^{-1}$ are also considered to reveal the strain rate effect.

III. RESULTS AND DISCUSSION

We first discuss how the plastic flow stress (strength) depends on the grain size with a focus on the strength softening regime (inverse Hall–Petch effect). The inset of Fig. 1(c) presents the flow stress variation over grain size in the BNG structures. It can be seen that the stress increases with a decrease in the grain size, but starting from 14 nm, the stress shows a plateau, followed by a gradual declining trend. To understand the influence of bimodal structure in the strength softening, we compare the flow stresses and grain size curve of BNG with that of HNG, as shown in Fig. 1(c). It is of interest to note that the softening rate of BNG is considerably lower as compared with HNG structures, which suggests a strength softening alleviation enabled by grain size heterogeneity (i.e., bimodal grain size distribution).

To reveal the source of strength behind the mitigation of softening in BNG structures, we compute the flow stresses of small and large grains, and their variations with small grain size are plotted in Fig. 1(d). With a decrease in the small grain size, the small grains exhibit a loss of strength. Intriguingly, the large grains show a clear increase in strength. This strength increase in large grains balances the strength reduction of small grains, which is the root cause of softening alleviation of BNG systems.

Before discussing the fundamental mechanisms that are responsible for the strength increase of large grains, we begin with the introduction of the stress-strain responses and the underlying deformation processes in BNG structures. Figures 2(a)-2(c) show the stress-strain curves for small and large grains in BNG structures with different small grain sizes of 14, 9, and 2 nm, respectively. It is evident that the curves are separating from one another with a decrease in the small grain size from 12 to 2 nm, exhibiting an increasing strength of large grains and a decrease in small ones. This strength increases in large grains, benefiting from reducing the small grain size, suggests a strengthening mechanism originated from the bimodal structure. For small grains, the stress overshoot (yielding drop) keeps reducing, and for the small grain size of 2 nm, the stress drop vanished. This is because with a decrease in the grain size, the predominant plastic deformation mechanism responsible for yielding is changing from dislocation nucleation to grain boundary-mediated sliding.²⁰ In Figs. 2(d)-2(e), we show the deformed structures for BNG with small grain sizes, 14 and 9 nm, respectively. At 3% applied strain, the 9 nm small grains show dislocation emission from grain boundary, while the 14 nm grains remain elastic. At the beginning of the plastic flow stage (5% strain), more dislocations are activated in the small grains, and the large grains start to deform plastically. Large grains undergo increased dislocation slip during plastic flow (at 15% strain), and

we find that more dislocations are stored in large grains with reducing the small grain size (see discussion of Fig. 4).

Next, we analyze and compare the strained structures, local plastic strain, and boundary sliding of BNG and HNG, aiming to understand the effect of bimodal structure on deformation mechanisms, intragranular slip, and grain boundary activities. In the left panels of Fig. 3, we present the deformed configurations at 15% strain for BNG with the small grain size of 6 nm, HNG 20 nm, and HNG 6 nm. As indicated by the red-colored atoms, deformation mechanisms like partial slip, twinning, and stacking fault are triggered. Unlike dislocation slip and twinning that can be described by affine deformation field, grain boundary activities such as sliding and migration are more of a nonaffine atomic rearrangement. $D_i^2 = \sum_{j=1}^{n_i} |\mathbf{d}_{ij} - \mathbf{J}_i \mathbf{d}_{ij}^0|^2$, to quantify grain boundary deformation, where \mathbf{d}_{ij} is the distant vector from atom i to its neighbor atom j in the current state and \mathbf{d}_{ii}^0 is for the initial state, and \mathbf{J}_i is affine deformation tensor that transforms a nearest neighbor separation, \mathbf{d}_{ii}^0 , to what would be expected under an affine deformation. By minimizing D_i^2 , one can obtain the best J_i and thus local shear strain η^{2} Here, local atomic strain η , acting as the invariant of the local strain tensor, can better describe intragranular plastic deformation due to dislocation slip. The middle and right panels of Fig. 3 show the spatial distributions of local strain η and non-affine displacement D_i^2 , respectively. It is noteworthy that, in the shear strain maps, there are more plastic slips (denoted in the figure) in the grain interior of bimodal structure than that of homogeneous structure. This means dislocations have passed over that large grain region multiple times, indicating enhanced transgranular plasticity in BNG structures. From a grain boundary viewpoint, one can see that the non-affine displacement (grain boundary sliding) associated with grain boundaries in bimodal structures is smaller than their homogeneous counterparts. This reduction in grain boundary sliding suggests that the large grains are stabilized by the surrounding small grains, which is considered to be the cause for enhanced dislocation slip.

To further reveal the deformation behaviors of BNG, we extend the deformation simulations at a wide range of strain rates from 1×10^{10} to 5×10^7 /s. Figure 4(a) shows the plastic flow stress changes with respect to the variation of strain rate for HNG 20 nm and BNG 14 nm. By comparing the values (slope) of strain rate sensitivity m, it is evident that BNG is less sensitive to strain rate variation and its flow stress drop is less than that of homogeneous one within the same variation of strain rate. However, previous studies claimed that with a decrease in the mean grain size, there will be an increase in the strain rate sensitivity due to improved grain boundary sliding. ^{23,24} To elucidate the surprisingly reduced strain rate sensitivity of BNG, we extract and compare the total lengths of different dislocation types in the BNG 14 nm and HNG 20 nm, as shown in Fig. 4(b). Their spatial distributions of dislocation are illustrated in Figs. 4(d) and 4(e), respectively. The BNG system, even if has half the volume of small grains, exhibits a high density of dislocations than the homogeneous structure with all large grains of 20 nm. Specifically, as the primary dislocation types that govern plastic slip in low stacking fault energy metals, the total length of Shockley partial dislocation²⁵ and the total length of sessile stair-rod dislocation, 26 which is formed by the reaction of

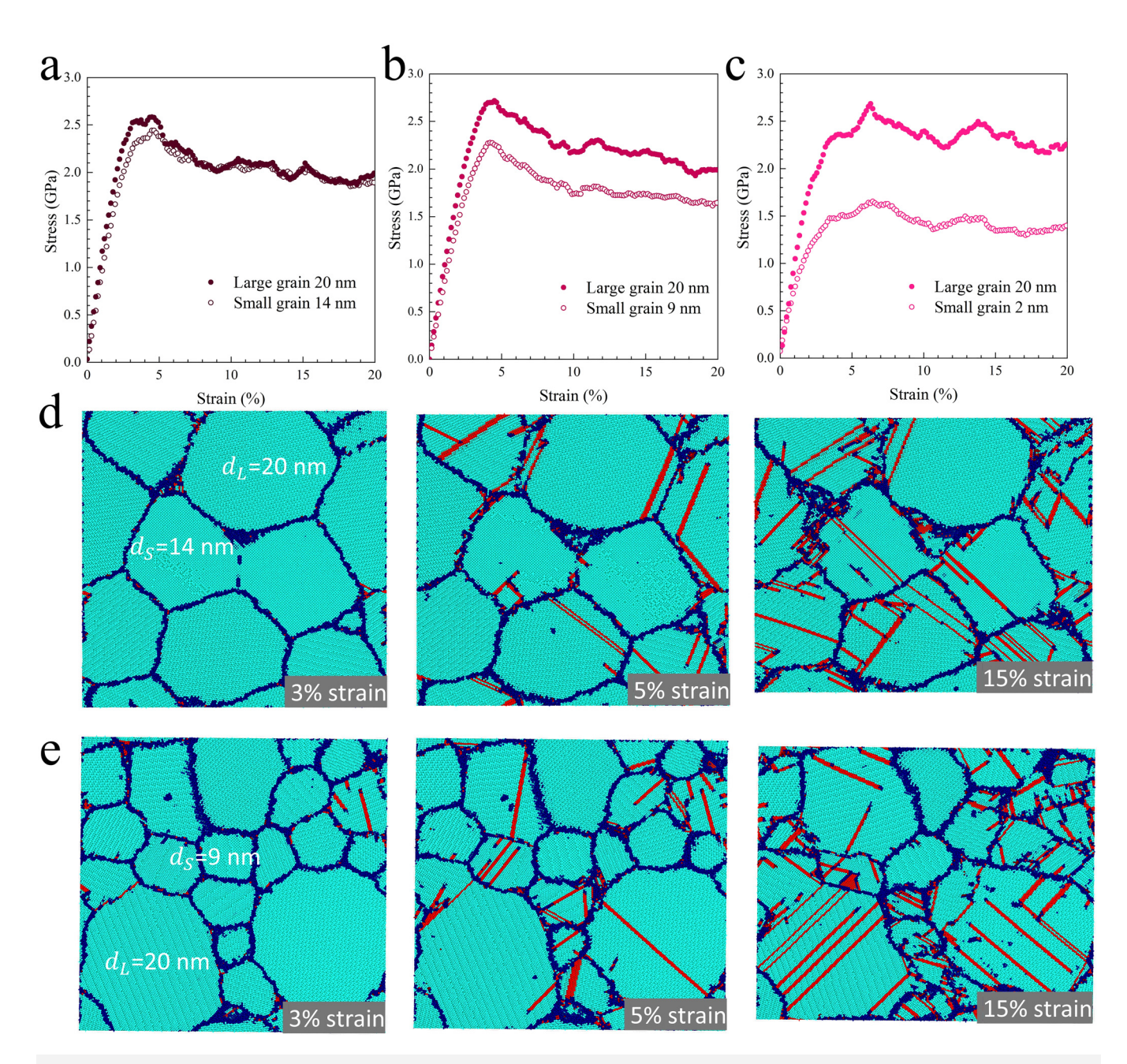


FIG. 2. Strain-stress curves of BNG structures with small grain sizes of (a) 14 nm (b) 9 nm, and (c) 2 nm. Solid circles and hollow circles denote large grains and small grains, respectively. By reducing the size of small grain, the stress of large grain is increasing. (d)–(e) Deformed BNG structures at 3% (upon yielding), 5% (at the initial stage of plastic flow), and 15% (during plastic flow) applied strain with small grain size of (d) 14 nm and (e) 9 nm. The dark blue and red colors represent grain boundary atoms and HCP atoms, respectively.

two Shockley partials, are both higher in the BNG 14 nm, which may be responsible for the excessive strength of the BNG. In Fig. 4(c), we demonstrate the fractions of different atom types and the calculated mean nonaffine squared displacement $\langle D_{\min}^2 \rangle$ in the two

systems. By analyzing the structural types, atoms constituting defects, such as dislocation, twin boundary, and stacking fault, are categorized as defective or displaced atoms. Unlike the HNG structure, the fact that the percentage of the slipped atoms is higher in

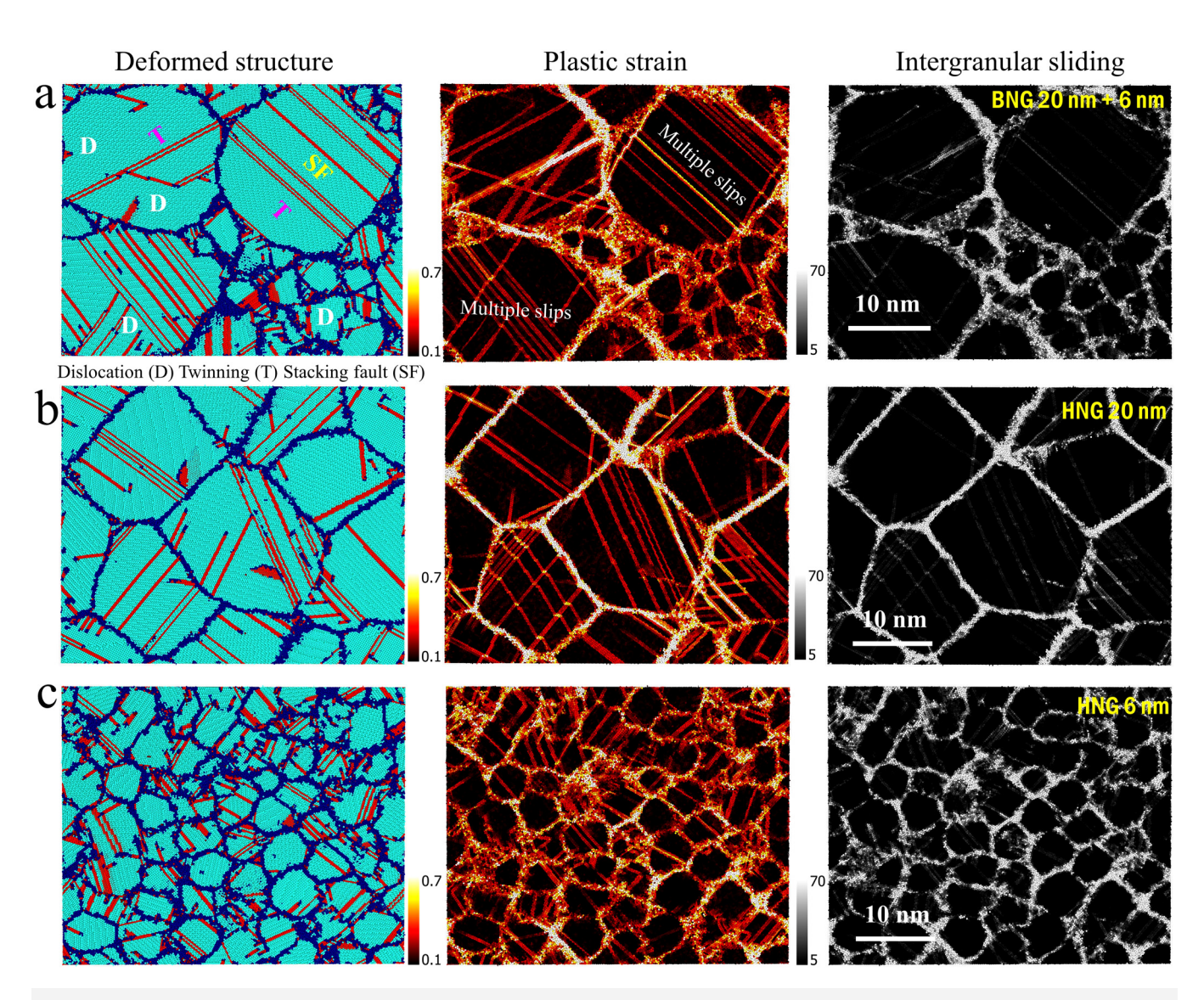


FIG. 3. Plastic deformation mechanisms illustrated by deformed structure (dislocation, twinning, and stacking fault are denoted by D, T, and SF), local atomic shear strain (grain interior slip history), and the nonaffine squared displacement (grain boundary sliding). (a) BNG structure with a small grain size of 6 nm. (b)–(c) Homogeneous structures with a grain size of (b) 20 nm and (c) 6 nm.

the BNG structure indicates the promoted plasticity. It is noteworthy that, even if the percentage of grain boundary atoms is higher in the BNG system (i.e., grain boundaries take a larger portion of the volume in the BNG), these grain boundaries experience less sliding compared to HNG system, as indicated by the reduced value of $\langle D_{\min}^2 \rangle$. As a result of diminished grain boundary activities and possible structure stabilization, the dislocation slip and the transgranular plastic deformation, especially in the large grains, are promoted. One noteworthy point is that the strain rate in our MD simulations is several orders of magnitude higher than that in normal experiments. With sufficiently decreasing strain rate, thermally activated diffusional processes, such as vacancy-mediated

dislocation climb, can take place and overcome the dislocation obstacles, decreasing the plastic flow stresses. Because the HNG structures have lower dislocation storage (fewer pinning points), it is reasonable to speculate that the HNG will experience fast strength drop with a decrease in the strain rate compared with BNG systems.

IV. CONCLUSION

This study manifests a nontrivial effect of grain size nonuniformity on the mechanical behavior of nanograined structures. It is found that the softening rate in the inverse Hall–Petch regime

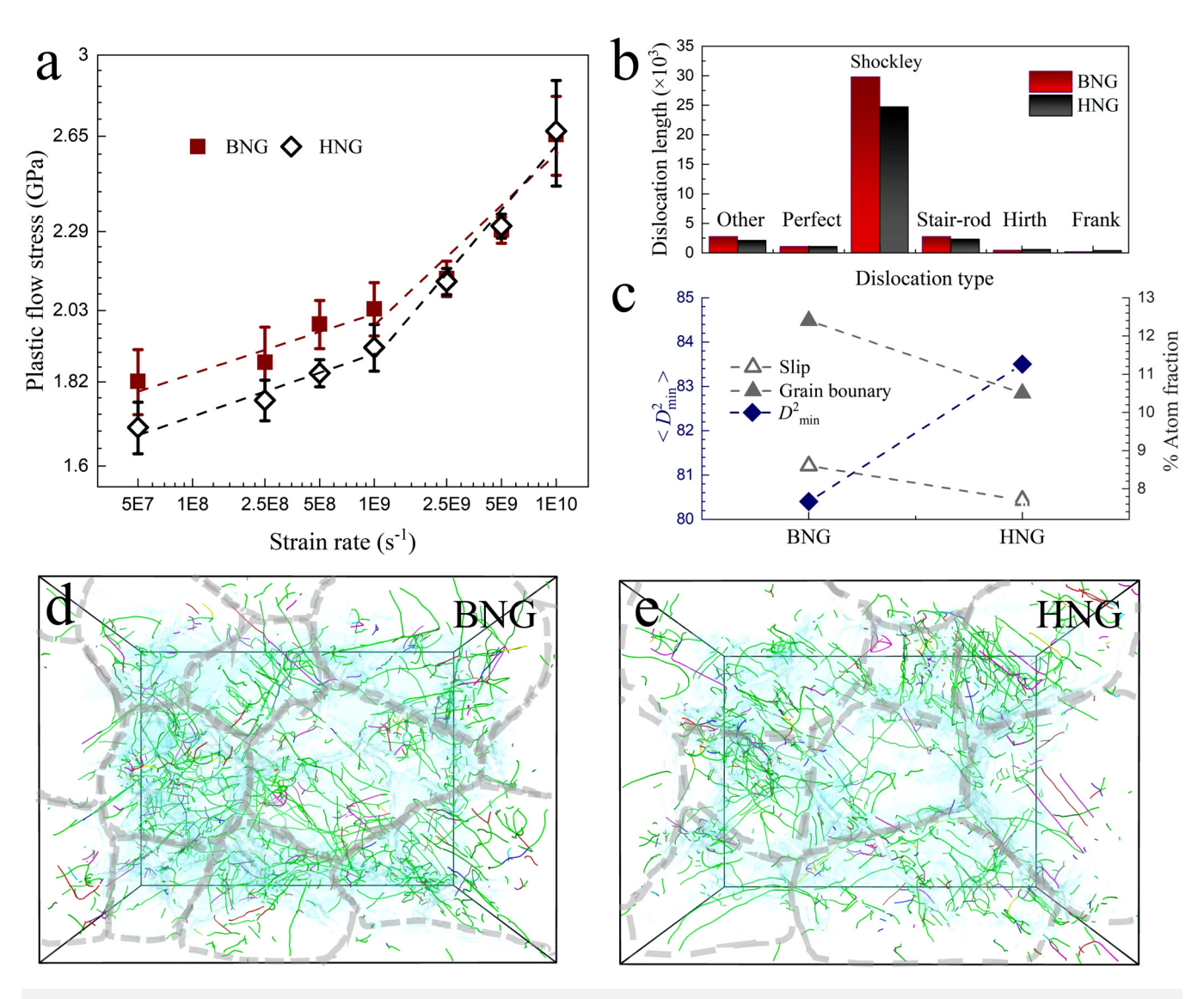


FIG. 4. (a) Double logarithmic plot of plastic flow stress as a function of strain rate for BNG (square) and HNG (diamond). (b) The dislocation length of different types of dislocations in NBG and HNG. (c) Nonaffine squared displacement and the fractions of different atom types for BNG and HNG structures. (d)–(e) The spatial dislocations of dislocations in bimodal structure and homogeneous structure, deformed to 20% applied strain. Data are obtained from structures deformed at a strain rate of $5 \times 10^7/s$. The dislocations are colored by type: Perfect (royal blue), Shockley (green), Stair-rod (pink), Hirth (yellow), Frank (light blue), and Other (red). The gray line indicates grain boundary.

can be tailored and alleviated by tuning structural heterogeneity (grain size uniformity). Specifically in the bimodal nanostructured metals, the mitigation of strength softening is enabled by the enhanced plasticity of large grains and diminished grain boundary sliding process. Extra dislocation nucleation and storage are believed to contribute to the ultrahigh strengthening in a broad class of heterogeneous structured materials. During mechanical deformation, dislocation gliding and pileup can be formed at the vicinity of grain boundaries, resulting in stress concentration. In consequence, a back-stress pointing to the dislocation source could

act as a strengthening mechanism. When the stress concentration at a grain boundary reaches a threshold value, dislocation slip in the neighboring grains can be activated, enhancing the dislocation slip. With a decrease in the grain size, it becomes more difficult to trigger the slip systems in the confined grain region,³ and it increases the threshold value of stress concentration at the grain boundary in large grains, thus, allowing more dislocation pileups, which is a strengthening mechanism in metals.^{3,30} In the heterogeneously structured materials, the unusual structure packing with many small grains encompassing large grains may promote

dislocation slip in both grains. An extensive dislocation slip in the large grains could produce geometrically necessary dislocations to accommodate the deformation incongruity between large and small grains.^{27,29,31} Our results of revealing softening rate alleviation in the inverse Hall–Petch regime enabled by tailoring grain size non-uniformity shed light on the fundamental deformation mechanisms in emergent heterogeneous structures.

ACKNOWLEDGMENTS

H.W., and P.C. acknowledge support from National Science Foundation under grant number DMR-2105328.

AUTHOR DECLARATIONS

Conflict of Interest

The authors have no conflicts to disclose.

DATA AVAILABILITY

The data that support the findings of this study are available from the corresponding author upon reasonable request.

REFERENCES

- ¹E. O. Hall, "The deformation and ageing of mild steel: III. Discussion of results," Proc. Phys. Soc. B **64**, 747–753 (1951).
- ²R. Song, D. Ponge, D. Raabe, J. G. Speer, and D. K. Matlock, "Overview of processing, microstructure and mechanical properties of ultrafine grained bcc steels," Mater. Sci. Eng. A 441, 1–17 (2006).
- ³N. Hansen, "Hall-Petch relation and boundary strengthening," Scr. Mater. 51, 801–806 (2004).
- ⁴M. Chandross and N. Argibay, "Ultimate strength of metals," Phys. Rev. Lett. 124, 125501 (2020).
- ⁵F. H. Duan, Y. Naunheim, C. A. Schuh, and Y. Li, "Breakdown of the Hall–Petch relationship in extremely fine nanograined body-centered cubic Mo alloys," Acta Mater. 213, 116950 (2021).
- ⁶H. Somekawa and T. Mukai, "Hall–Petch breakdown in fine-grained pure magnesium at low strain rates," Metall. Mater. Trans. A **46**, 894–902 (2015).
- ⁷J. Schioøtz and K. W. Jacobsen, "A maximum in the strength of nanocrystalline copper," Science 301, 1357–1359 (2003).
- ⁸Y. Wei, A. F. Bower, and H. Gao, "Enhanced strain-rate sensitivity in fcc nanocrystals due to grain-boundary diffusion and sliding," Acta Mater. 56, 1741–1752 (2008).
- ⁹E. Ma and T. Zhu, "Towards strength-ductility synergy through the design of heterogeneous nanostructures in metals," Mater. Today 20, 323–331 (2017).
- 10Y. Wang, M. Chen, F. Zhou, and E. Ma, "High tensile ductility in a nanostructured metal," Nature 419, 912–915 (2002).
- ¹¹Y. Zhao, T. Topping, J. F. Bingert, J. J. Thornton, A. M. Dangelewicz, Y. Li, W. Liu, Y. Zhu, Y. Zhou, and E. J. Lavernia, "High tensile ductility and strength in bulk nanostructured nickel," Adv. Mater. 20, 3028–3033 (2008).

- ¹²X. Li, L. Lu, J. Li, X. Zhang, and H. Gao, "Mechanical properties and deformation mechanisms of gradient nanostructured metals and alloys," Nat. Rev. Mater. 5, 706–723 (2020).
- ¹³N. Tsuji, Y. Ito, Y. Saito, and Y. Minamino, "Strength and ductility of ultrafine grained aluminum and iron produced by ARB and annealing," Scr. Mater. 47, 893–899 (2002).
- ¹⁴X. Wu and Y. Zhu, "Heterogeneous materials: A new class of materials with unprecedented mechanical properties," Mater. Res. Lett. **5**, 527–532 (2017).
- 15Y. Zhao, Y. Zhu, and E. J. Lavernia, "Strategies for improving tensile ductility of bulk nanostructured materials," Adv. Eng. Mater. 12, 769–778 (2010).
- ¹⁶X. Wu, M. Yang, F. Yuan, G. Wu, Y. Wei, X. Huang, and Y. Zhu, "Heterogeneous lamella structure unites ultrafine-grain strength with coarse-grain ductility," Proc. Natl. Acad. Sci. U.S.A. 112, 14501–14505 (2015).
 ¹⁷S. M. Foiles, M. I. Baskes, and M. S. Daw, "Embedded-atom-method functions
- ¹⁷S. M. Foiles, M. I. Baskes, and M. S. Daw, "Embedded-atom-method functions for the fcc metals Cu, Ag, Au, Ni, Pd, Pt, and their alloys," Phys. Rev. B 33, 7983–7991 (1986).
- ¹⁸S. Nosé, "A molecular dynamics method for simulations in the canonical ensemble," Mol. Phys. **52**, 255–268 (1984).
- ¹⁹W. G.Hoover, "Canonical dynamics: Equilibrium phase-space distributions," Phys. Rev. A 31, 1695–1697 (1985).
- ²⁰P. Cao, "The strongest size in gradient nanograined metals," Nano Lett. 20, 1440–1446 (2020).
- ²¹P. Cao, M. P. Short, and S. Yip, "Understanding the mechanisms of amorphous creep through molecular simulation," Proc. Natl. Acad. Sci. U.S.A. 114, 13631–13636 (2017).
- ²²F. Shimizu, S. Ogata, and J. Li, "Theory of shear banding in metallic glasses and molecular dynamics calculations," Mater. Trans. 48, 2923–2927 (2007)
- ²³Q. Wei, S. Cheng, K. T. Ramesh, and E. Ma, "Effect of nanocrystalline and ultrafine grain sizes on the strain rate sensitivity and activation volume: Fcc versus bcc metals," Mater. Sci. Eng., A 381, 71–79 (2004).
- ²⁴J. Chen, L. Lu, and K. Lu, "Hardness and strain rate sensitivity of nanocrystal-line Cu," Scr. Mater. 54, 1913–1918 (2006).
- 25 J. Wang and H. Huang, "Shockley partial dislocations to twin: Another formation mechanism and generic driving force," Appl. Phys. Lett. 85, 5983–5985 (2004).
- ²⁶V. Yamakov, D. Wolf, S. R. Phillpot, and H. Gleiter, "Dislocation-dislocation and dislocation-twin reactions in nanocrystalline Al by molecular dynamics simulation," Acta Mater. 51, 4135–4147 (2003).
- ²⁷J. Bach, M. Stoiber, L. Schindler, H. W. Höppel, and M. Göken, "Deformation mechanisms and strain rate sensitivity of bimodal and ultrafine-grained copper," Acta Mater. 186, 363–373 (2020).
- ²⁸Y.-J. Wang, A. Ishii, and S. Ogata, "Transition of creep mechanism in nanocrystalline metals," Phys. Rev. B 84, 224102 (2011).
- ²⁹Z. Zeng, X. Li, D. Xu, L. Lu, H. Gao, and T. Zhu, "Gradient plasticity in gradient nano-grained metals," Extreme Mech. Lett. 8, 213–219 (2016).
- ³⁰H. Yu, Y. Xin, M. Wang, and Q. Liu, "Hall-Petch relationship in Mg alloys: A review," J. Mater. Sci. Technol. **34**, 248–256 (2018).
- 31H. Gao and Y. Huang, "Geometrically necessary dislocation and size-dependent plasticity," Scr. Mater. 48, 113–118 (2003).